DE-Vol. 84-2, 1995 Design Engineering Technical Conferences
Volume 3 — Part B
ASME 1995

CRITICAL SPEEDS RESULTING FROM UNBALANCE EXCITATION OF BACKWARD WHIRL MODES

Lyn M. Greenhill
Rotordynamics–Seal Research
North Highlands, CA

Guillermo A. Cornejo
Power Systems Engineering Division
Solar Turbines
San Diego, CA

ABSTRACT

Most rotordynamic analyses typically ignore the potential for critical speeds to be created by traversing a backward precessional whirl mode. While not commonly recognized, a backward mode can be excited using unbalance as the driving force. Based on the analysis of a Jeffcott rotor-bearing model, it was found that the condition for this response to occur is strongly dependent on stiffness asymmetry in the rotordynamic coefficients at the supports. To illustrate the application of this result, a rotordynamic analysis on actual hardware is presented, in which the unbalance excited backward mode resonance is calculated to occur. Test data is also given indicating the presence of the predicted critical speed. It is important to note that although the resonance is due to the backward mode, the precessional direction is forward. Several recommendations are offered with respect to rotor-bearing design so that this unique critical speed situation may be avoided.

INTRODUCTION

When considering the synchronous critical speeds of rotor-bearing systems, the majority of attention in both the technical literature and practical design has been focused on the unbalance excitation of natural frequencies with whirling and spinning in the same direction. This has not received much interest lately, judging from the age of several definitive works in this area, such as Lund and Orcutt (1967); Kirk and Gunter (1972); Barrett, Gunter, and Allaire (1978). The lack of recent literature is not unwarranted, since the motion, which is commonly referred to as forward precession, is driven by the unbalance force which contains a vector component oriented in the direction of rotation. Common intuition leads most analysts to conclude that since unbalance produces a forward precessional force, only modes that are whirling in the same direction should be considered for potential synchronous excitation.

A recent rotordynamics analysis of a large, fluid-film bearing supported generator, however, predicted a synchronous critical speed to occur as a result of exciting a ***backward*** precessional mode. After the analysis, the generator was acceptance tested, at which time excitation of the backward mode critical speed was postulated. It should be noted that in both the analysis and testing, the rotor precessional direction was forward, although the natural frequency causing the resonance was a backward mode. To the authors' knowledge, only Vance (1988) has postulated that unbalance can excite backward modes, and then only if the modes are "planar" in displaced shape.

NOMENCLATURE

C_{xx} = X-axis bearing direct damping
C_{xy} = X-Y plane cross-coupled damping
C_{yy} = Y-axis bearing direct damping
C_{yx} = Y-X plane cross-coupled damping
K_{xx} = X-axis bearing direct stiffness
K_{xy} = X-Y plane cross-coupled stiffness
K_{yy} = Y-axis bearing direct stiffness
K_{yx} = Y-X plane cross-coupled stiffness
I_d = rotor diametral (transverse) inertia
I_p = rotor polar (longitudinal) inertia
M = rotor mass
l_1 = axial distance from bearing 1 to rotor mass
l_2 = axial distance from bearing 2 to rotor mass
t = time variable
X = inertial reference transverse displacement of rotor mass
Y = inertial reference transverse displacement of rotor mass

As a result of encountering this surprising critical speed, a detailed analytical investigation is presented to characterize the rotordynamic parameters that can produce an unbalance excited backward mode resonance. To simplify the analysis, a Jeffcott rotor supported on general linear bearings was used. All of the common rotordynamic coefficients, including direct and cross-coupled terms, were evaluated in the analysis for the potential to create this unique critical speed. The analysis of and test data from the machine which exhibited the backward mode resonance are also given. This paper concludes with some recommendations and guidelines for avoiding such critical speeds.

THEORETICAL DEVELOPMENT

In the generator example analysis, it was found that the predominate influence on the synchronous unbalance excitation of the backward mode was support properties. With a large, flexible rotordynamics model such as used in the generator analysis, it is difficult to isolate quantitatively the influence of the support coefficients on the critical speed response. As such, a standard Jeffcott rotor-bearing model was used to develop the relationships between rotordynamic coefficients and predicted response.

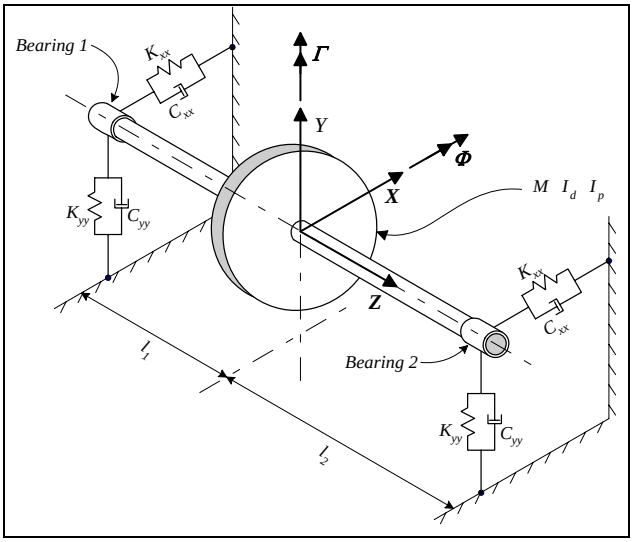

FIGURE 1. SINGLE MASS RIGID ROTOR SUPPORTED ON GENERAL LINEAR BEARINGS

The Jeffcott model used in this theoretical development is illustrated in Figure 1. A fixed *XYZ* inertial reference frame measuring absolute displacement from the bearing centerline is used to describe motions of the system, with the *Z*-axis oriented in the axial direction. For use with unbalance, a rotating *xyz* reference frame is also used, with the *z*-axis coincident with the *Z*-axis, and the *x*- and *y*-axes fixed to the disk, rotating at constant angular velocity Ω. The rotor is considered to be rigid, with the entire system inertia concentrated at the centrally located disk. The position of the disk was allowed to vary axially between the two bearings by the distances l_1 and l_2, as illustrated in the figure.

Considering only steady-state motion, and with the rigid rotor assumption, the system possesses 4 degrees-of-freedom. These system variables are illustrated in Figure 1, and referred to as *X* and *Y* for the transverse orthogonal displacements from the bearing centerline, and Φ and Γ for rotational motion about the rotor mass. Forces at each of the bearings were represented by full stiffness and damping matrices consisting of both direct and cross-coupled terms, although the figure only illustrates direct terms. Due to the use of the general bearing representations, motion in the *X*-*Y* as well as in the *X*-*Z* and *Y*-*Z* planes is fully coupled. A complete presentation of the system equations of motion is given in the Appendix.

For the purposes of this theoretical development, both the homogeneous eigenvalue and harmonic forced response problems given by equation (A-6) in the Appendix were solved using standard techniques. To maintain generality, the results for all combinations of support parameters are given using non-dimensional notation such as α for stiffness ratio and β for cross-coupled stiffness ratio (see the Nomenclature section for complete definition of all symbols). All bearing coefficients were held constant over the values of speed ratio considered.

The initial configuration considered by this analysis is the completely symmetric, isotropic, lightly damped system that has natural frequency characteristics illustrated in Figure 2. Although four modes should be generated, only three are shown, as the first two modes are identically equal in frequency for this case. These modes are the first two cylindrical or bounce modes. Due to the frequency ratio definition, a possible critical speed is predicted at a speed ratio of unity for such modes. The third and fourth modes are conical or pitching modes, with maximum displacement at each bearing and no motion at the rotor mass. These modes also illustrate the influence of gyroscopic effects, in that the frequencies change with increasing speed ratio. The

NOMENCLATURE

$\alpha = K_{yy}/K_{xx}$ = direct stiffness ratio

$\beta = K_{xy}/K_{xx} = K_{yx}/K_{yy}$ = cross-coupled stiffness ratio

δ = unbalance response maximum displacement

ε_x, ε_y, ε_z = unbalance eccentricities in rotating *xyz* reference frame

Φ = rotational displacement of rotor mass about *X*-axis

Γ = rotational displacement of rotor mass about *Y*-axis

$\lambda = l_1/l_2$ = rotor mass axial position ratio

Ω = rotor spin speed

$\omega_x = \sqrt{\frac{K_{xx}}{M}}$ = *X*-axis undamped natural frequency

$\omega_y = \sqrt{\frac{K_{yy}}{M}}$ = *Y*-axis undamped natural frequency

$\zeta_x = \frac{\omega_x C_{xx}}{2K_{xx}}$ = *X*-axis direct damping ratio

$\zeta_y = \frac{\omega_y C_{yy}}{2K_{yy}}$ = *Y*-axis direct damping ratio

values of polar and diametral inertia were chosen for this example such that a possible synchronous critical speed at a speed ratio of 2.2 is predicted for the backward third mode. The forward fourth mode is not expected to have any potential synchronous critical speeds over the speed ratio range of interest.

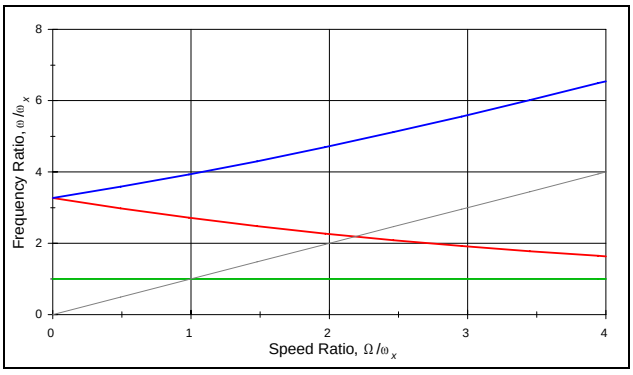

FIGURE 2. NATURAL FREQUENCY MAP FOR SYMMETRIC, ISOTROPIC JEFFCOTT SYSTEM

Using unbalance eccentricities of $\varepsilon_x = 1$, $\varepsilon_y = 0$, and $\varepsilon_z = 10$ (which correspond physically to center of mass offsets), the unbalance response of this symmetric system was determined. The relatively large axial eccentricity was chosen purposely to excite the backward pitching mode, if possible.

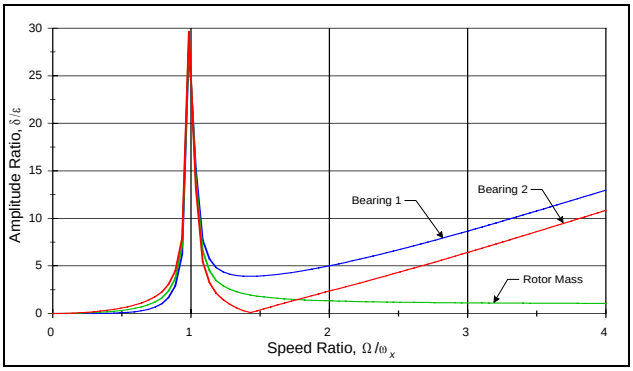

FIGURE 3. UNBALANCE RESPONSE FOR ISOTROPIC, SYMMETRIC JEFFCOTT SYSTEM

Figure 3 displays the response calculated in terms of an amplitude ratio, which is the maximum displacement at the bearings and rotor mass divided by the vector combination of the radial eccentricities. Note that for this case, the combination is simply equal to the ε_x eccentricity. Direct damping values equal to 1% of critical ($\zeta_x = \zeta_y = .01$) were applied to the system to limit peak response.

As is commonly expected, the unbalance response shown in Figure 3 indicates a sharp, lightly damped resonance at a speed ratio near unity. The amplitudes at each bearing are not equal due to the added axial eccentricity, which introduces a moment about the rotor mass. Note that the crossing of the backward mode at a speed ratio of 2.2 produces no resonance.

The modal characteristics and unbalance response illustrated in Figures 2 and 3 are typically reported for most analysis of the Jeffcott rotor. However, the purpose of the theoretical development presented in this paper was to investigate the atypical aspects of the Jeffcott system. The primary variables that were studied in order to determine the effect on the response of a general rotor-bearing system were:

- Direct stiffness asymmetry (values of $\alpha \neq 1$)
- Direct damping (changes in ζ_x and ζ_y)
- Cross-coupled stiffness (values of $\beta \neq 0$)
- Rotor mass asymmetry (values of $\lambda \neq 1$)

Each of these four characteristics will be discussed in the following separate sections. While not directly analyzed, cross-coupled damping can be expected to act similarly to direct stiffness, since the forces produced by each term are in the same direction.

Direct Stiffness Asymmetry

Keeping the same values of mass eccentricity and damping ratios, the direct stiffness coefficients at each bearing were modified to orthotropic values. For the purposes of this study, values of α from 1.0 to 3.0 were considered. Figure 4 displays the natural frequency map that is produced for $\alpha = 2.0$, which is a common proportion of asymmetry for rotors supported in fluid film bearings.

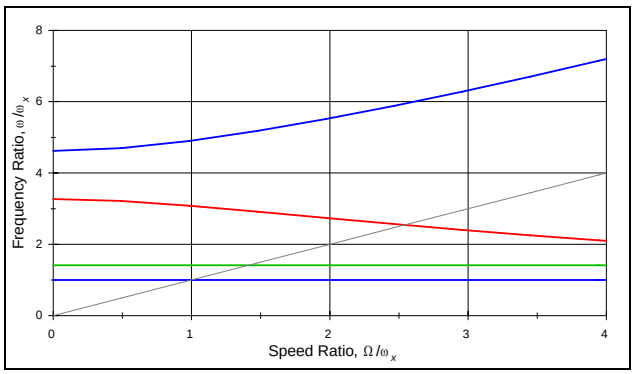

FIGURE 4. NATURAL FREQUENCY MAP FOR JEFFCOTT SYSTEM WITH $\alpha = 2.0$

Compared to Figure 2, the orthotropic bearing system now separates the first two modes as well as the forward and backward pitching modes. Three potential synchronous critical speeds can result from this system, at speed ratio values of 1.0, 1.4, and 2.5. Using the same eccentricities as the isotropic case, the unbalance response for the orthotropic system is shown in Figure 5. As the figure illustrates, a dramatic difference in response is evident, compared with Figure 3. Most notably, a strong resonance is now predicted at the 2.5 speed ratio, which is the backward mode synchronous crossing, with the motion predominately at the two bearings. As a result of incorporating bearing stiffness asymmetry, synchronous unbalance excitation of the backward mode has created a significant resonance.

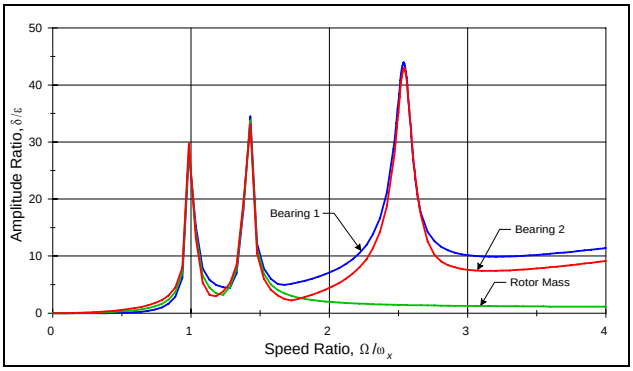

FIGURE 5. UNBALANCE RESPONSE FOR JEFFCOTT SYSTEM WITH $\alpha = 2.0$

Confirmation of the backward mode excitation is also given by examining the precessional direction of the whirl orbits. For the system response shown in Figure 5, the orbit is backwards between the first two criticals and in the vicinity of the third (from speed ratios approximately 2.3 to 3.0). At all other speed ratios, the precession direction is forward. The backward whirl between the first two criticals is discussed in Vance (1988). The retrograde precession on both sides of the third critical speed has not, to the authors' knowledge, been presented in the technical literature, and is due to the point mass assumption used with the Jeffcott model. It was noted that the transition from forward to backward whirl, and vice versa, occurs at speed ratios with highly elliptical orbits.

Certainly, the mechanism by which unbalance can excite backward modes is relatively straightforward – if the backward mode is "planar" enough, then ***any*** source of excitation will create a resonance. The key aspect of this behavior is how "planar" the mode must be in order to be driven. A comparison of the normalized displacements at the bearings and rotor mass at the backward mode resonant speed ratio is given in Table 1 for the range of α values considered in this analysis.

TABLE 1. BACKWARD MODE NORMALIZED ORBITS AS A FUNCTION OF STIFFNESS ASYMMETRY

Asymmetry (α)	Speed Ratio Ω/ω_x	Bearing 1 Orbits		Rotor Mass Orbits		Bearing 2 Orbits	
		Major	Minor	Major	Minor	Major	Minor
1.0	2.20	1.00	-1.00	0.00	0.00	1.00	-1.00
1.1	2.22	1.00	-0.97	0.00	0.00	1.00	-0.95
1.5	2.40	1.00	-0.69	0.00	0.00	1.00	-0.69
2.0	2.54	1.00	-0.53	0.00	0.00	1.00	-0.53
3.0	2.71	1.00	-0.37	0.00	0.00	1.00	-0.37

Reviewing the orbits in Table 1, it is obvious that the backward mode is far from "planar," yet significant response is produced even at relatively low values of asymmetry. In fact, for the relatively simple Jeffcott rotor-bearing system considered in this study, it was found that ***any*** amount of asymmetry in the direct stiffness coefficients would create a backward mode resonance excited by unbalance.

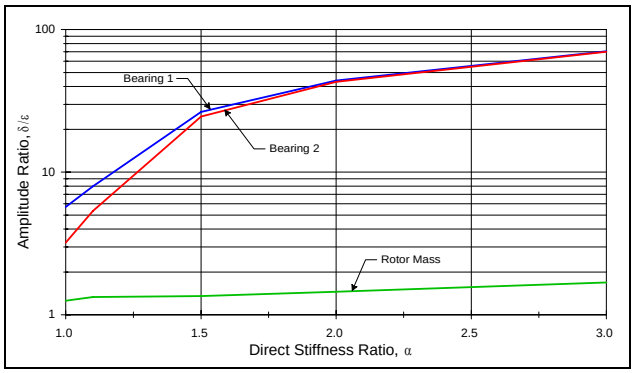

FIGURE 6. AMPLITUDE RATIOS AT BACKWARD MODE AS A FUNCTION OF STIFFNESS ASYMMETRY

For values of α equal to 1.0 to 3.0, Figure 6 displays the peak amplitude ratios predicted from unbalance response at the backward mode resonance. As shown in Figure 6, the effect of asymmetry is immediate, and more pronounced as larger values of α are used. Notice that the motion at the rotor mass is largely unaffected by the asymmetry, due to the pitching displacement of the mode shape.

Direct Damping

Arguably, the amount of damping used in the asymmetry calculations is relatively low. It may be postulated that for reasonable amounts of damping, the backward mode resonance will be attenuated. Using the same values of mass eccentricity as with the stiffness asymmetry studies, damping ratio values were increased to 5 percent. The direct stiffness coefficients at each bearing were set to values corresponding to $\alpha = 2.0$, and the resulting unbalance response is displayed in Figure 7.

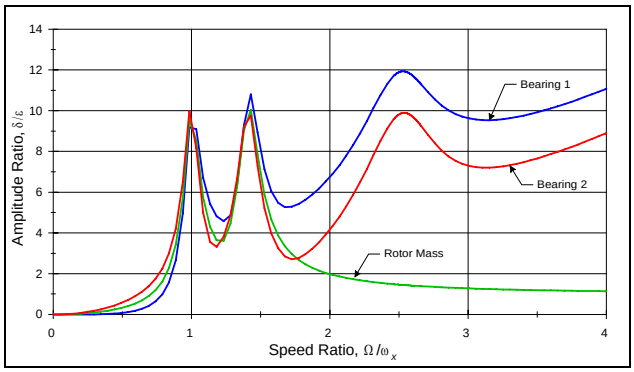

FIGURE 7. EFFECT OF INCREASED DAMPING ($\zeta_X = \zeta_Y = 5\%$) ON UNBALANCE RESPONSE ($\alpha = 2.0$)

As anticipated, using the constant damping coefficients in this study, the effect of increasing the amount of damping on the higher frequency backward mode is significant. With larger values of damping, the backward mode resonance can be overdamped and the critical speed eliminated. It should be noted, however, that in practice, damping coefficients tend to decrease as speed increases, especially with fluid film bearings.

Cross-Coupled Stiffness

While stability is not an issue in this analysis, it is an important consideration in the design of supercritical machinery. By opposing damping, cross-coupled stiffness creates a tangential force that could also alter the response produced in the previous section. Values of the cross-coupled stiffness parameter β from 0.1 to 1.0 were applied to the $\alpha = 2.0$ asymmetric system with damping ratios held at 1 percent.

The cross-coupled coefficients were added to the system stiffness matrix in a skew symmetric fashion, i. e., $K_{yx} = -K_{xy}$, which is the common sign convention used with these terms. As expected, a slight change in system stability was observed at high speed ratios, however, the most notable affect of the increasing cross-coupling was to reduce the frequency difference between the first two cylindrical modes as the value of the cross-coupling ratio β was increased. The amplitude and speed ratio value of the backward mode resonance was largely unchanged for the range of β considered. Figure 8 displays the unbalance response for the condition of β equal to unity, that is, the cross-coupled coefficients equal to the magnitude of the direct terms.

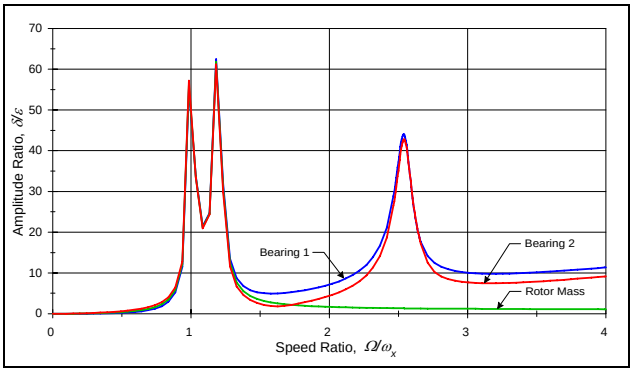

FIGURE 8. EFFECT OF CROSS-COUPLED STIFFNESS ($\beta = 1$) ON ASYMMETRIC UNBALANCE RESPONSE

Compared to Figure 5, the separation of the first two critical speeds has decreased, while the amplitude has increased significantly. This response is due to the implicit shift in principle stiffness directions as a result of the cross-coupled coefficient magnitudes. The shift reduces the effective amount of asymmetry by coupling the response in both lateral planes. Amplitudes at the first two critical speeds have increased because the amount of direct damping is also reduced by the opposing force created by the cross-coupled stiffness coefficients. The backward mode resonance, however, is practically unchanged. The influence of cross-coupled stiffness is not as significant for this mode, due to the inherently larger amount of damping available as a result of the constant damping coefficient assumption.

Rotor Mass Asymmetry

The final parameter investigated with the Jeffcott rotor model is the influence of the position of the rotor mass. Typically, the Jeffcott model places the disk equidistant from each bearing. However, the system analyzed here specifically did not place this constraint on the formulation of the equations of motion. This generalization was made in order to determine if the backward mode resonant response is peculiar result of rotor symmetry, since as Table 1 listed, the participation of the rotor mass is minimal with this mode.

With the $\alpha = 2.0$ asymmetric system and 1% damping ratios, the axial position parameter λ was changed from unity to 3.0, which increases and correspondingly decreases the distance between the rotor mass and bearings 1 and 2 by 50%, respectively. The unbalance response of this system is illustrated in Figure 9.

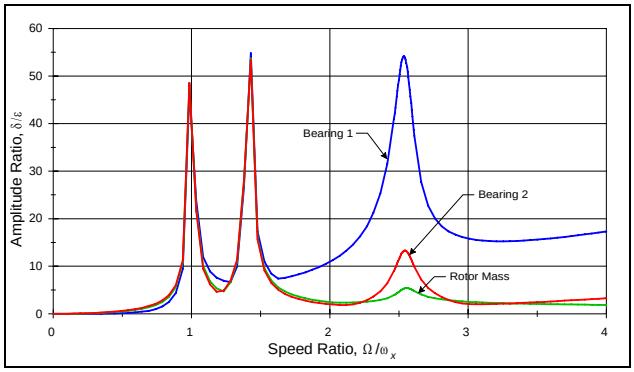

FIGURE 9. EFFECT OF ROTOR MASS ASYMMETRY ($\lambda = 3$) ON UNBALANCE RESPONSE ($\alpha = 2$)

With the rotor mass now unsymmetric axially, a disproportionate moment is created at bearing 1, as shown in Figure 9. Compared with Figure 5, more motion is created at the mass, with less displacement at bearing 2, which is closer to the unbalance forces. Based on the results of this response, it can be concluded that with respect to the backward mode critical speed, the use of an axially symmetric system does not create a unique configuration that is particularly sensitive to bearing asymmetry.

EXAMPLE ROTOR ANALYSIS

The main impetus for the entire theoretical development of the previous section was to explain the analytical and empirical observations obtained from an actual piece of rotating machinery. This particular machine was a horizontal generator, operating at 1800 rpm, with a rotor 120 inches long weighing 8500 lbm, and the center of gravity nearly at the rotor midpoint. Figure 10 displays a plot of the rotor geometry used to analyze the dynamics of the rotor-bearing system. The actual rotor model was adjusted geometrically to match frequencies obtained from free-free modal testing. In addition to the geometry, Figure 10 also displays the location of the two bearings.

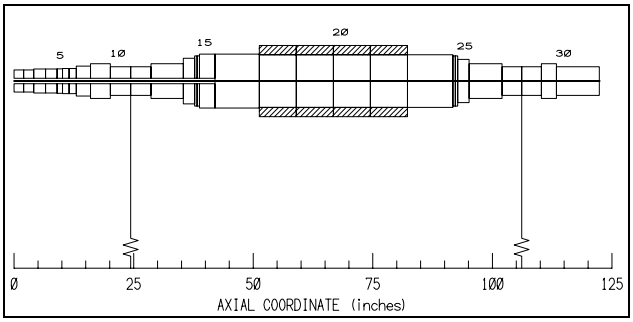

FIGURE 10. GEOMETRY MODEL OF GENERATOR ROTOR EXAMPLE

The rotor was supported by fluid film bearings, which were in turn mounted on pedestals that are significantly stiffer in the vertical direction than horizontal. The combination of the static bearing load and the pedestal mounting stiffnesses produced a relatively asymmetric effective support for the rotor. Using measured values of horizontal and vertical pedestal stiffness, and calculated coefficients for the fluid film bearings, Tables 2 and 3 list the combined effective coefficients used in the subsequent rotordynamic analysis, for the operating speed of 1800 rpm.

TABLE 2. GENERATOR ROTOR EXAMPLE EFFECTIVE STIFFNESS COEFFICIENTS AT 1800 RPM

K_{xx} (N/m)	K_{xy} (N/m)	K_{yx} (N/m)	K_{yy} (N/m)
1.005×10^8	-1.979×10^7	-2.732×10^7	1.905×10^8

TABLE 3. GENERATOR ROTOR EXAMPLE EFFECTIVE DAMPING COEFFICIENTS AT 1800 RPM

C_{xx} (N-sec/m)	C_{xy} (N-sec/m)	C_{yx} (N-sec/m)	C_{yy} (N-sec/m)
1.506×10^5	-7.005×10^5	2.102×10^5	2.785×10^5

Reviewing the coefficients in Table 2, note that the direct stiffness is asymmetric, with a stiffness ratio $\alpha = 2$ approximately. As listed in Table 3, the supports provide adequate damping, with damping ratios of $\zeta_x = 12\%$ and $\zeta_y = 16\%$, and stiffness cross-coupling is low. It should be noted that the coefficients given in Tables 2 and 3 are for the operating speed of 1800 rpm only, since with fluid film bearings, the dynamic properties are speed dependent.

Natural frequency characteristics for the generator rotor are illustrated in Figure 11. Only three modes occur in the frequency range up to 4000 cpm.

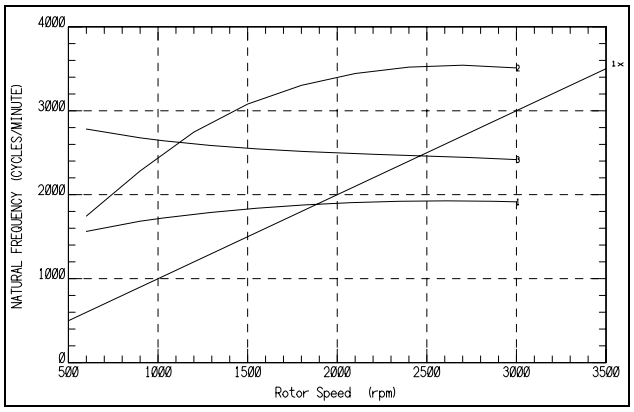

FIGURE 11. NATURAL FREQUENCY MAP FOR GENERATOR ROTOR EXAMPLE

The first mode, which is illustrated in Figure 12 at 1800 rpm, is a forward cylindrical mode, with a potential synchronous critical speed at nearly 1900 rpm. This mode is well damped, however, with a log decrement of almost unity. With such a large amount of damping, excitation of such a mode would not produce significant amplitudes.

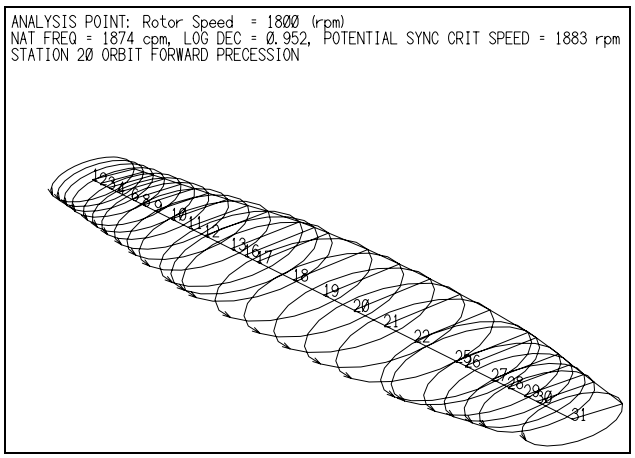

FIGURE 12. FIRST MODE SHAPE OF GENERATOR ROTOR EXAMPLE

The second mode in the natural frequency map is a forward conical mode, and due to the speed dependent properties of the supports, never crosses the synchronous operating line. The third natural frequency, shown in Figure 13, is a backward cylindrical

mode, with a predicted synchronous critical speed near 2500 rpm. The log decrement of this mode is almost 0.6, which can be considered adequate damping. Note that both modes with synchronous crossing display elliptical orbits, due to the direct stiffness asymmetry, although the third mode is more "planar" than the first, and that the whirl direction of each mode, as shown by the arrows on the mode shape plots, are in opposite directions.

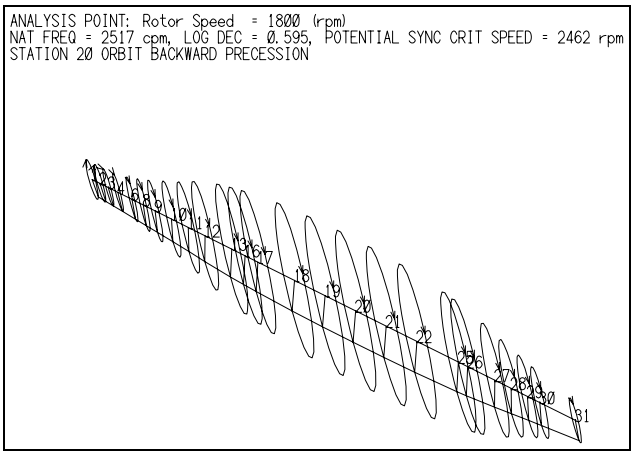

FIGURE 13. THIRD MODE SHAPE OF GENERATOR ROTOR EXAMPLE

Using a cylindrical unbalance distribution, the unbalance response of the generator rotor was calculated, for which a typical displacement plot is shown in Figure 14. Two mild yet distinct peaks are produced, corresponding to the synchronous crossing of the first ***and*** third modes. Notice that the minor axis amplitude changes sharply before the third mode resonance peak, which was observed in the Jeffcott rotor analysis.

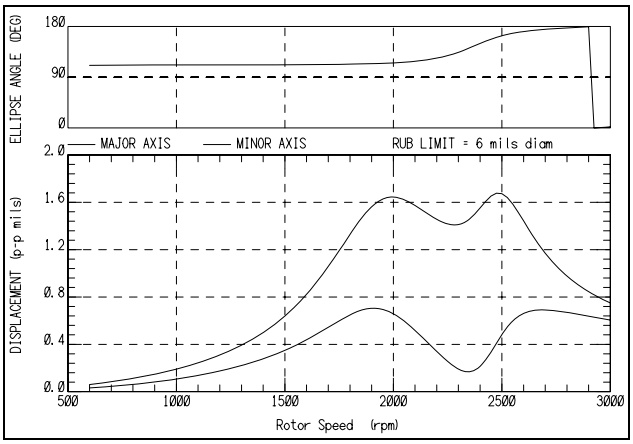

FIGURE 14. TYPICAL UNBALANCE RESPONSE OF GENERATOR ROTOR EXAMPLE

Unlike the Jeffcott rotor example, the generator rotor does not exhibit any backward precession when traversing the backward mode. Response shapes for the rotor at 1800 and 2400 rpm are illustrated in Figures 15 and 16. Note the precessional direction is forward in each plot, although the relative ellipticity is markedly higher at 2400 rpm. This difference in response is attributed to a more uniform distribution of rotor mass, rather than lumping at one point in the Jeffcott model, and the flexible shaft representation used in the generator analysis.

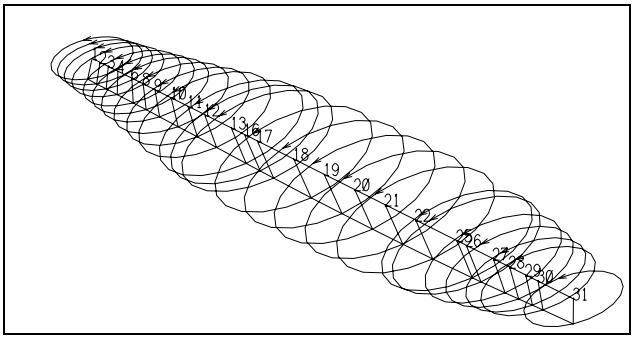

FIGURE 15. GENERATOR ROTOR EXAMPLE RESPONSE SHAPE AT 1800 RPM

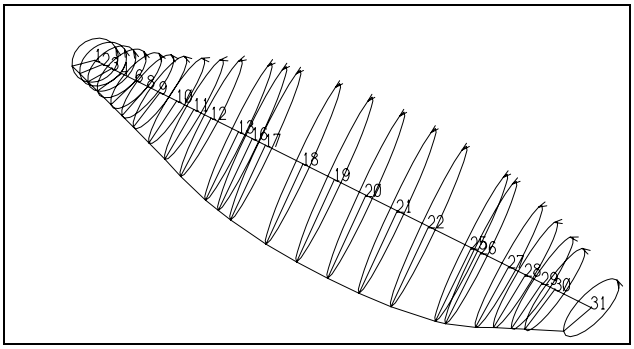

FIGURE 16. GENERATOR ROTOR EXAMPLE RESPONSE SHAPE AT 2400 RPM

The fundamental source of the backward mode excitation, as postulated with the Jeffcott analysis, was confirmed with the generator rotor example to be stiffness asymmetry. It was found that if the direct stiffness coefficients, as listed in Table 2, were made equal, the backward mode excitation would not occur. No attempt to parametrically vary the coefficients was made, since at the time of the analysis, it was considered that if the backward mode resonance was present, sufficient margin over operating speed existed.

EXPERIMENTAL VALIDATION

During acceptance testing of the generator, several different values of unbalance and oil temperature were used in an attempt to "map" response. Normally during this procedure, the unit is run over design speed to establish critical speed margins. Since the first mode was heavily damped near operating speed, the third or backward mode was the only resonance that might be found over design speed. The objective of the testing was to verify that the first mode would not create any problem vibration, and determine if the backward mode could be excited.

The first piece of data obtained during testing is shown in Figure 17. In this bode plot, the amplitude and phase at one of the bearings is displayed as a function of speed. Displacements at the other bearing were similar. The particular test was with cold oil and no added unbalance weights (i. e., residual rotor unbalance only). As the figure shows, the resonance at 1800 rpm is not evident, being well damped as expected. Unfortunately, the maximum speed attainable was 2250 rpm, which is short of the peak response due to the backward mode crossing (see Figure 14). However, some type of resonance is clearly being excited, or the response would not build so steeply above 1800 rpm.

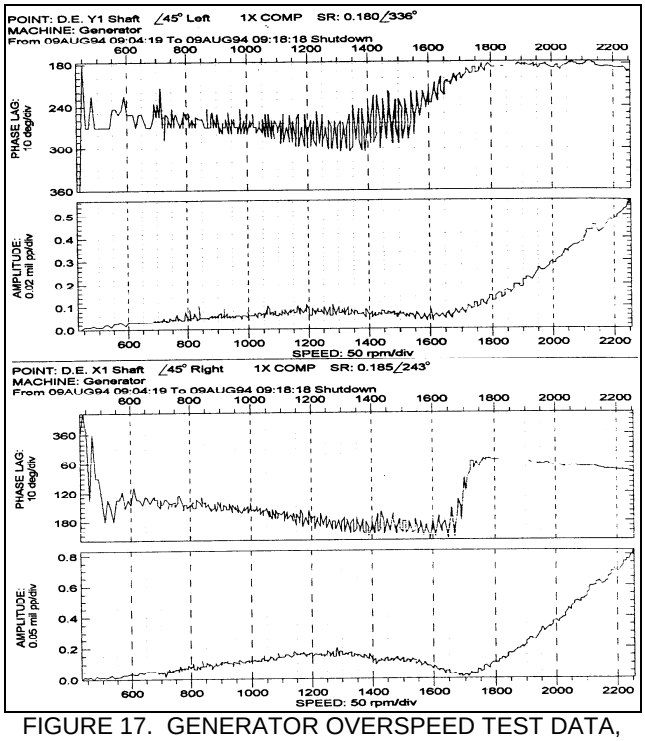

FIGURE 17. GENERATOR OVERSPEED TEST DATA, COLD OIL, NO UNBALANCE WEIGHTS

Notice in Figure 17 that the phase plots indicate the presence of some dynamic phenomenon at roughly 1700 rpm. The amplitudes in each direction are not equal, indicating some ellipticity to the orbit, as would be expected from the analysis.

The next piece of data taken during overspeed testing is shown in Figure 18, illustrating the response of the generator with hot oil. With the increased oil temperature, the natural frequencies should decrease, due to lower viscosity.

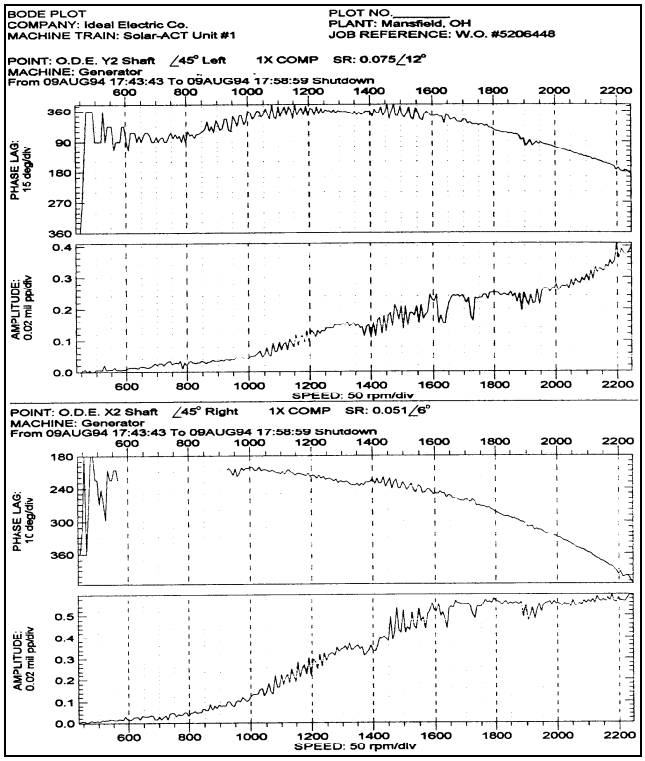

FIGURE 18. GENERATOR OVERSPEED TEST DATA, HOT OIL, NO UNBALANCE WEIGHTS

In Figure 18, the amplitudes with hot oil are lower, and the sudden rise in response above 1800 rpm is not present. The first mode is more evident, with increasing amplitude above 2000 rpm, perhaps indicating the onset of the backward mode.

Figure 19 presents the last set of data, corresponding to cold oil with unbalance weights. This data confirms the location of the first mode, at approximately 1900 rpm, although the response is well damped. The amplitude in each direction is not equal, implying elliptical orbits. Above the first mode, the response is decaying, however, the machine could not be oversped high enough to positively confirm the backward mode. Although not shown, response similar to Figure 19 was obtained with hot oil.

Reviewing the data given in Figures 17 through 19, the presence of the backward mode can neither be confirmed or denied. What can be said is that the data gives the impression that a mode is present above 2250 rpm, and based on the analysis, it was concluded that this resonance is due to the backward mode. Obviously, more substantial test data is needed before the backward mode excitation can be proven.

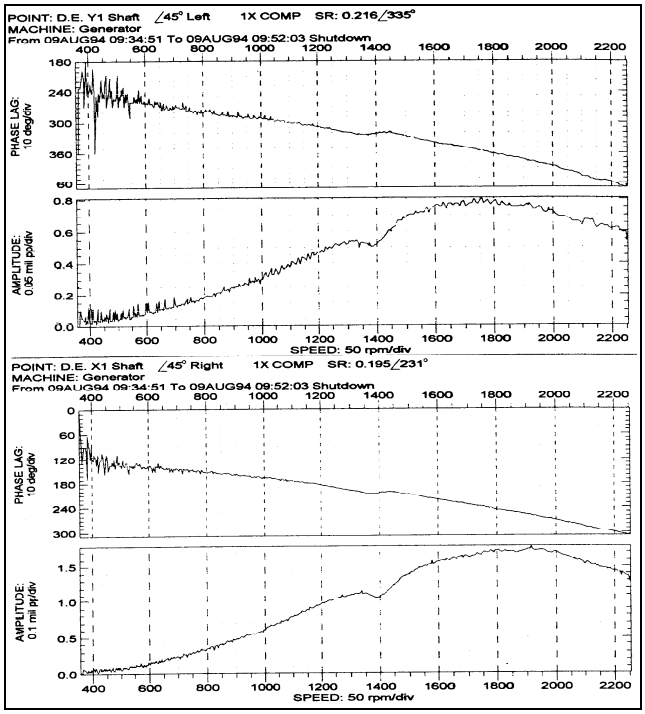

FIGURE 19. GENERATOR OVERSPEED TEST DATA, COLD OIL, WITH UNBALANCE WEIGHTS

SUMMARY AND CONCLUSIONS

Based upon the results of a typical natural frequency analysis on a fluid film bearing supported rotor system, a unique resonance condition was encountered. A critical speed was produced by the unbalance excitation of a backward precessional mode. To the authors' knowledge, this phenomenon has not been significantly discussed in the technical literature, and has certainly not been quantified.

In order to more fully understand this critical speed, an enhanced Jeffcott model utilizing rotatory degrees of freedom and general linear bearing representations was used to characterize the rotordynamic parameters that create such a resonance. Based on the study, it was found that:

- By far the most significant influence on the presence of the backward mode excitation is direct stiffness asymmetry. With the Jeffcott analysis, small differences in the magnitude of direct stiffness terms generated the backward mode resonance. In an analysis of a typical rotor-bearing system, changing the calculated asymmetric supports to a system with equal direct stiffness terms eliminated the predicted backward mode resonance.
- Increasing direct damping reduces the peak amplitude of the backward mode resonance, as would be expected.
- Cross-coupled stiffness does not appreciably alter the backward mode resonance.
- While not directly investigated, cross-coupled damping should behave in a manner similar to direct stiffness, since the forces produced by both act in the same direction.

Based on these findings, it can be recommended that to avoid exciting backward modes, asymmetry in the direct stiffness terms should be avoided. Of course, this usually not practical, especially with fluid film bearings. Fortunately, the large amount of damping available with such bearings tends to overdamp backward modes, thus eliminating the potential resonance. It can be stated, however, that if rotor supports create direct stiffness asymmetry, the potential for unbalance excitation of backward modes does exist, and should be considered in any analysis.

Test data taken from a machine with a predicted backward mode resonance indicated the presence of the critical speed, although the data was not completely definitive. It would be extremely useful to confirm the backward mode resonance with data taken from a test rig or other suitable experimental rotor-bearing system.

REFERENCES

Barrett, L. E., Gunter, E. J., and Allaire, P. E., 1978, "Optimum Bearing and Support Damping for Unbalance Response and Stability of Rotating Machinery," *Journal of Engineering for Power*, Trans. ASME, Vol. 100, pp. 89-94.

Childs, D., 1993, Turbomachinery Rotordynamics, John Wiley.

Ehrich, F. E., editor, 1992, Handbook of Rotordynamics, McGraw-Hill.

Gunter, E. J., 1966, Dynamic Stability of Rotor-Bearing Systems, NASA SP-113.

Jeffcott, H. H., 1919, "The Lateral Vibrations of Loaded Shafts in the Neighborhood of a Whirling Speed: The Effect of Want of Balance," *Philosophy Magazine*, Ser. 6, Vol. 37, pp. 304.

Kirk, R. G., and Gunter, E. J., 1972, "The Effect of Support Flexibility and Damping on the Synchronous Response of a Single-Mass Flexible Rotor," *Journal of Engineering for Industry*, Trans. ASME, Vol. 94, pp. 221-232.

Lund, J. W., and Orcutt, F. K., 1967, "Calculations and Experiments on the Unbalance Response of a Flexible Rotor," *Journal of Engineering for Industry*, Trans. ASME, Vol. 89, pp. 785-796.

Vance, J. M., 1988, Rotordynamics of Turbomachinery, John Wiley.

APPENDIX – JEFFCOTT ROTOR-BEARING SYSTEM EQUATIONS OF MOTION

A centrally located mass mounted between two supports for the investigation of rotordynamic behavior has been used extensively in the technical literature. For example, Childs (1993), Ehrich (1992), Vance (1989), and even Gunter (1966) make extensive use of this model to illustrate basic phenomena. The earliest recognized analysis of this system is attributed to Jeffcott (1919), whose name is commonly used to refer to this type of model.

For the critical speed investigation in this paper, a more general Jeffcott model was required than is normally developed, specifically, a system that can produce backward modes and accommodate general linear bearings. In order to create retrograde precession natural frequencies, it is necessary to include gyroscopic effects, which in turn requires rotational degrees-of-freedom. The use of general linear bearings is primarily a constraint on the method of solution, since the fundamental equations of motion will no longer be uncoupled.

The rotor-bearing equations of motion were developed using the Lagrangian approach, modeling rotor kinetic energy and bearing generalized forces. Using small angle approximations and dropping high order terms, the kinetic energy T of the rotor can be written as

$$T = \tfrac{1}{2}M(\dot{X}^2+\dot{Y}^2)+\tfrac{1}{2}[I_p(\Omega^2-2\dot{\Gamma}\Omega\Phi)+I_d(\dot{\Gamma}^2+\dot{\Phi}^2)] \quad \text{(A-1)}$$

where Ω is the rotor spin speed. Taking the prescribed Lagrangian derivatives of (A-1) results in a set of system equations, which may be expressed in matrix form as

$$\begin{bmatrix} M & 0 & 0 & 0 \\ 0 & M & 0 & 0 \\ 0 & 0 & I_d & 0 \\ 0 & 0 & 0 & I_d \end{bmatrix}\begin{Bmatrix} \ddot{X} \\ \ddot{Y} \\ \ddot{\Phi} \\ \ddot{\Gamma} \end{Bmatrix} - \Omega\begin{bmatrix} 0 & 0 & 0 & 0 \\ 0 & 0 & 0 & 0 \\ 0 & 0 & 0 & -I_p \\ 0 & 0 & +I_p & 0 \end{bmatrix}\begin{Bmatrix} \dot{X} \\ \dot{Y} \\ \dot{\Phi} \\ \dot{\Gamma} \end{Bmatrix} = \{Q\} \quad \text{(A-2)}$$

or $$[M]\{\ddot{q}\} - \Omega[G]\{\dot{q}\} = \{Q\}$$

in which the generalized coordinates in (A-2) are given by $\{q\}$ and the generalized forces by $\{Q\}$. The unspecified generalized forces are obtained from virtual work.

The expression for the lateral force applied to a rotor by a general linear bearing is

$$\{F_b\} = -\begin{bmatrix} K_{xx} & K_{xy} \\ K_{yx} & K_{yy} \end{bmatrix}\begin{Bmatrix} X_b \\ Y_b \end{Bmatrix} - \begin{bmatrix} C_{xx} & C_{xy} \\ C_{yx} & C_{yy} \end{bmatrix}\begin{Bmatrix} \dot{X}_b \\ \dot{Y}_b \end{Bmatrix} \quad \text{(A-3)}$$

where the subscript b in (A-3) indicates the motion of the rotor at the bearing. Because of the rotational degrees of freedom, the displacements at the bearings must also include angular components. The transformation from motion at the rotor mass to each bearing is given by

$$\begin{aligned} X_1 &= X - l_1\Gamma & X_2 &= X + l_2\Gamma \\ Y_1 &= Y + l_1\Phi & Y_2 &= Y - l_2\Phi \end{aligned} \quad \text{(A-4)}$$

with the subscripts *1* and *2* in (A-4) denoting bearings 1 and 2, respectively. With the bearing forces from (A-3), and the displacements from (A-4), with velocities obtained from the time derivative of displacements, virtual work expressions may be formed for each bearing. The virtual work terms may then be equated directly to generalized forces in (A-2). A typical expression for the generalized force is illustrated by the spring component of

$$-\{Q_K\} = \left[\begin{array}{c|c} [K^{UL}] & [K^{UR}] \\ \hline [K^{LL}] & [K^{LR}] \end{array}\right]\begin{Bmatrix} X \\ Y \\ \Phi \\ \Gamma \end{Bmatrix} \quad \text{(A-5)}$$

in which the submatrix stiffness components are

$$[K^{UL}] = \begin{bmatrix} (K_{1xx}+K_{2xx}) & (K_{1xy}+K_{2xy}) \\ (K_{1yx}+K_{2yx}) & (K_{1yy}+K_{2yy}) \end{bmatrix} \quad \text{(A-5a)}$$

$$[K^{UR}] = \begin{bmatrix} (l_1K_{1xy}-l_2K_{2xy}) & (-l_1K_{1xx}+l_2K_{2xx}) \\ (l_1K_{1yy}-l_2K_{2yy}) & (-l_1K_{1yx}+l_2K_{2yx}) \end{bmatrix} \quad \text{(A-5b)}$$

$$[K^{LL}] = \begin{bmatrix} (l_1K_{1yx}-l_2K_{2yx}) & (l_1K_{1yy}-l_2K_{2yy}) \\ (-l_1K_{1xx}+l_2K_{2xx}) & (-l_1K_{1xy}+l_2K_{2xy}) \end{bmatrix} \quad \text{(A-5c)}$$

$$[K^{LR}] = \begin{bmatrix} (l_1^2K_{1yy}+l_2^2K_{2yy}) & (-l_1^2K_{1yx}-l_2^2K_{2yx}) \\ (-l_1^2K_{1xy}-l_2^2K_{2xy}) & (l_1^2K_{1xx}+l_2^2K_{2xx}) \end{bmatrix} \quad \text{(A-5d)}$$

where the rotordynamic coefficients for each bearing are treated distinctly as indicated by the subscripts. In the force expression of (A-5), note that the matrix may not be symmetric, and the influence of rotatory effects. In most developments of a Jeffcott rotor-bearing system, even if rotational degrees of freedom are considered, the effect of rotation is not included.

For damping, a similar generalized force to (A-5) may be constructed, with the stiffness replaced by damping coefficients, and displacements replaced by velocities. The general system equation of motion can then be written as

$$[M]\{\ddot{q}\} + ([Q_C] - \Omega[G])\{\dot{q}\} + [Q_K]\{q\} = \{Q_U\} \quad \text{(A-6)}$$

where $[Q_C]$ is the damping generalized force and $\{Q_U\}$ is the unbalance force vector. Unbalance is incorporated by specifying three mass eccentricity values (ε_x , ε_y , ε_z) in a rotating *xyz* reference frame (which is attached to the rotor mass). The axial eccentricity produces a moment about the lateral axes, and is necessary to excite pitching-type modes. The rotating reference forces and moments can be transformed to the fixed inertial *XYZ* system, which results in an unbalance vector expressed as

$$\{Q_U\} = M\Omega^2\begin{Bmatrix} \varepsilon_x\cos\Omega t - \varepsilon_y\sin\Omega t \\ \varepsilon_x\sin\Omega t + \varepsilon_y\cos\Omega t \\ \varepsilon_z(-\varepsilon_y\cos\Omega t - \varepsilon_x\sin\Omega t) \\ \varepsilon_z(-\varepsilon_y\sin\Omega t + \varepsilon_x\cos\Omega t) \end{Bmatrix} \quad \text{(A-7)}$$

where t is the time variable. Inserting (A-7) into (A-6) yields the complete system equations of motion.